Entropy-Driven Hydrogen Bonding: Stereodynamics of a Protonated, *N*,*N*-Chiral "Proton Sponge"

Paul Hodgson,[b] Guy C. Lloyd-Jones,*[a] Martin Murray,[a] Torren M. Peakman,[a] and Robert L. Woodward[a]

Abstract: The C_2-symmetric ("[DL]") and achiral ("[*meso*]") diastereoisomers of the hydrogen iodide salt of 1,8-bis-(*N*-benzyl-*N*-methylamino)naphthalene ([**2**H]$^+$[I]$^-$) interconvert in solution. Direct interconversion of the diastereoisomers of [**2**H]$^+$ must involve hydrogen bond fission (to give "[*non*HB-**2**H$^+$]") and rotation–inversion of the non-protonated nitrogen centre. The global activation parameters ($\Delta H^{\neq}$ and $\Delta S^{\neq}$) for diastereoisomer interconversion in [D_7]DMF have been determined from rate data obtained by temperature-drop and magnetisation-transfer ^{13}C NMR spectroscopy over a temperature range of 170 °C. The process is found to have a high entropy of activation in both directions ($\Delta S^{\neq} = 163(\pm 4)$ and $169(\pm 4)$ J K^{-1} mol^{-1}) and this is suggested to arise through hydrogen bonding of the ammonium centre in [*non*HB-**2**H$^+$] with the solvent ([D_7]DMF). Comparison of the enthalpy of activation ($\Delta H^{\neq}$) with that earlier found for diastereoisomer interconversion of the free-base form **2** suggests that the intramolecular hydrogen bond in [**2**H]$^+$ is roughly equal in enthalpic strength (ΔH) with that made with the solvent ([D_7]DMF) in the non-hydrogen-bonded intermediate [*non*HB-**2**H$^+$]. As such, the hydrogen bonding in [**2**H]$^+$ may be considered as predominantly an entropically driven process, without any unusual enthalpic strength.

Keywords: hydrogen bonds · isotopic labeling · NMR spectropscopy · proton sponges · stereodynamics

Introduction

Short, strong hydrogen bonds: Strong hydrogen bonds between donor "A–H" and acceptor "B" are generally accepted to be a predominantly covalent interaction with a bond energy in the range 10–40 kcal mol^{-1}.[1] These may be compared with weak and moderate hydrogen bonds where a much more electrostatic type interaction affords a bond energy in the range $\leq$4 kcal mol^{-1} (weak) and 4–10 kcal mol^{-1} (moderate). Strong hydrogen bonds are most often formed when there is a deficiency of electron density in the hydrogen-bond donor group, for example in "N$^+$–H$\cdots$B", or an excess of electron density in the acceptor group, for example, "O$^-\cdots$H–A" and are sometimes referred to as *ionic hydrogen bonds*. However, strong hydrogen bonds may also be formed intramolecularly when configurational or conformational effects force (neutral) donor and acceptor groups together. Jeffrey has suggested the term *forced strong hydrogen bonds* for these systems.[2] One may envisage that strong hydrogen bonding, occurring through both an *ionic* and *forced* interaction, may occur in the protonated form [**1a**H]$^+$ of the archetypal first generation[3] proton sponge[4] **1a**.

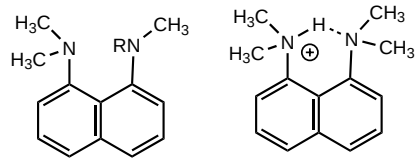

1a R = CH_3
1b R = H

[**1a**H]$^+$

There have been many calculations regarding the potential energy surface for the motion of a proton "H" between donor and acceptor "A" and "B" in a hydrogen-bond assembly "A–H$\cdots$B". At larger donor–acceptor distances, that is, "long hydrogen bonds", the potential energy surface consists of two minima with the deepest well on the coordinate closest to the donor "A". As the distance between acceptor and donor is reduced there is a narrowing in the shape of the potential energy surface and the barrier between the two minima is

[a] Dr. G. C. Lloyd-Jones, Dr. M. Murray, Dr. T. M. Peakman, R. L. Woodward
School of Chemistry
University of Bristol
Cantock's Close, Bristol BS8 1TS (UK)
Fax: (+44) 117-929-8611
E-mail: guy.lloyd-jones@bris.ac.uk

[b] Dr. P. Hodgson
Pfizer Ltd, Pfizer Central Research
Ramsgate, Kent, CT13 9NJ (UK)

 © WILEY-VCH Verlag GmbH, D-69451 Weinheim, 2000 0947-6539/00/0624-4451 $ 17.50+.50/0

reduced. Below a certain threshold acceptor–donor distance, the potential surface changes from being a double minimum to a low-barrier or no-barrier single minimum, resulting in a *low barrier hydrogen bond*. At this point, there is the minimum difference in zero-point energy between H and D, but on further decrease of acceptor–donor distance the difference in zero-point energy increases again as the single minimum potential narrows and steepens. However, since the switch from double potential well to a low-barrier symmetric system may occur at a donor–acceptor distance that results in moderately long bond lengths between the hydrogen and the donor and the acceptor, whether these are truly short strong hydrogen bonds is a matter of debate. As emphasised by Perrin and Nielson, the terms low-barrier hydrogen bond and short, strong hydrogen bond have been used interchangeably, even though the criteria used to recognise them are different.[5] Nonetheless, small isotopic fractionation factors (which are indicative of small difference in zero-point energy and thus a low barrier) have been used extensively to provide evidence for the generation of low barrier hydrogen bonds in enzyme catalysed biochemical reactions.[6] The presumed relationship between low-barrier and short, strong hydrogen bonds has also been used in proposals regarding the possible role of short, strong hydrogen bonds in providing stabilisation in enzyme–intermediate complexes.

Unsurprisingly, there is an ongoing and vivid debate regarding both the existence of short, strong hydrogen bonds in species that are in the solution phase (i.e. not in the gas phase) and their importance in enzymic catalysis.[7] Proponents[7a] and critics[7b] have, by necessity, entered into the discussion of very much simpler analogue species that are known or are assumed to have short, strong hydrogen bonds present when the system is solvated. The protonated proton sponge [**1a**H]$^+$ has been used extensively as an example of such a species.[7, 8]

The conclusion that there is a strong hydrogen bond in [**1a**H]$^+$ has been based on many observations including the remarkable basicity of **1a** (pK_a ca. 12, i.e. 10^6-fold more basic than **1b**),[3, 9] the identical electronegativity and polarisability of the two amine centres (i.e. $\Delta pK_a = 0$),[10] the very low field ^{1}H NMR shift of the hydrogen-bonded proton (ca. $\delta = 17-20$),[11] the intramolecular nature of the hydrogen bond, a very broad infra-red stretching band corresponding to the N–H bond,[3] the resistance of [**1a**H]$^+$ to further protonation ($\Delta[pK_{a1}pK_{a2}]$ ca. 20)[3] and low rates of proton exchange,[12] the identical N–H distances (1.31 Å) in some X-ray structures,[13, 14] low isotopic fractionation factors,[15] and more recently, high-level ab initio calculations.[16]

The relevance of [2H]$^+$ to the study of hydrogen bonding in proton sponges: We are currently engaged in the synthesis of chiral, first-generation proton sponges and recently we reported the protonated chiral proton sponge [**2**H]$^+$ (see Scheme 1) which has a stereogenic centre at both nitrogen atoms.[17] This salt exists as two diastereomers: chiral, C_2-symmetric-[(R_NR_N/S_NS_N)-**2**H]$^+$ ("[DL]-[**2**H]$^+$") and achiral [(R_NS_N)-**2**H]$^+$ ("[*meso*]-[**2**H]$^+$"). Because of protonation, the two amine stereogenic centres in [**2**H]$^+$ are "locked" together through what was predicted to be a short, strong hydrogen bond and hence this compound was expected to be stereochemically stable at the laboratory time scale at ambient temperature. However, [**2**H]$^+$ proved to be surprisingly stereolabile and thus the hydrogen bonding appeared significantly weaker than expected. Herein we report in full on the determination of activation parameters for the stereodynamic processes in [**2**H]$^+$ and compare these with those of its free base **2**. From this comparison, we draw conclusions regarding the strength of the hydrogen bonding in protonated proton sponges. Based on this we question the validity of the use of the protonated proton sponge [**1a**H]$^+$ as an example of a short, strong hydrogen bond relevant to enzymic catalysis.[7]

Results and Discussion

The surprising stereolability of [2H]$^+$: We have already reported the synthesis of [**2**H]$^+$[I]$^-$ by the neutral methylation of **3** (Scheme 1).[17] The stereochemical assignments of [DL]-[**2**H]$^+$[I]$^-$ and [*meso*]-[**2**H]$^+$[I]$^-$ in solution and solid state were based on isotopically desymmetrised NOE experiments and X-ray crystallography data.

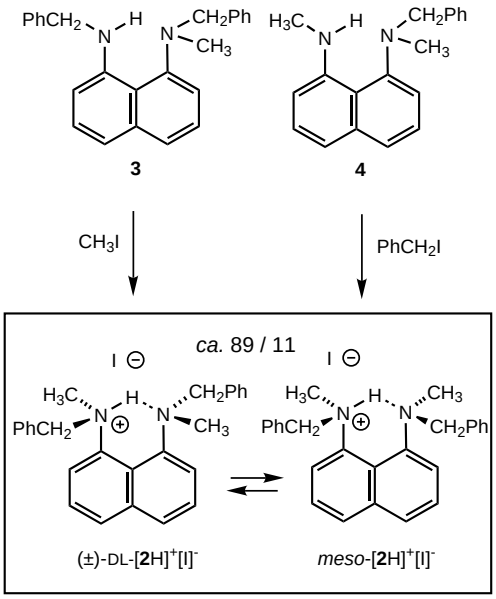

Scheme 1. The two routes employed in the synthesis of [**2**H]$^+$[I]$^-$.

We initially suspected significant stereolability of [**2**H]$^+$[I]$^-$ when we found that an alternative synthetic route to [**2**H]$^+$[I]$^-$ by neutral benzylation of **4** gave an identical diastereomeric ratio of [DL]-[**2**H]$^+$[I]$^-$ and [*meso*]-[**2**H]$^+$[I]$^-$ (ca. 88.5:11.5 at 25 °C). Subsequently, we found that large single crystals of [**2**H]$^+$[I]$^-$, which crystallises exclusively in the [DL] form, dissolved in CD_2Cl_2 at 25 °C to reproducibly give an 88.5:11.5 ratio of [DL]/[*meso*] diastereomers on ^{1}H NMR analysis within 10 minutes in solution. Thus, although the rate of equilibration of [DL] and [*meso*] isomers of [**2**H]$^+$[I]$^-$ is much slower than the NMR time scale (sharp NMR spectra are obtained) it is fast at the laboratory time scale.

© WILEY-VCH Verlag GmbH, D-69451 Weinheim, 2000
0947-6539/00/0624-4452 $ 17.50+.50/0 *Chem. Eur. J.* **2000**, *6*, No. 24

^{1}H and ^{2}H NMR shifts of the hydrogen-bonded proton: The magnitude of the ^{1}H NMR chemical shift, the primary hydrogen isotope effect ($\Delta\delta(^1H - ^2H)$ in ppm) on that shift and the isotopic fractionation factor of hydrogen-bonded systems can give information on the potential energy surface, the symmetry and the strength of the hydrogen bond. To obtain the primary hydrogen isotope effect value we prepared an approximately. 2:1 mixture of [**2**D]$^+$[I]$^-$ and [**2**H]$^+$[I]$^-$ by dissolving partially *N*-deuterated [D$_1$]-**3** in MeI. The $\Delta\delta(^1H - ^2H)$ values determined, at identical concentrations and temperatures for [DL]-[**2**H]$^+$[I]$^-$ and [*meso*]-[**2**H]$^+$[I]$^-$ in CD_2Cl_2 and CH_2Cl_2, respectively, were identical at 0.80 ppm. This, along with the chemical shifts ($\delta(^1H)(CD_2Cl_2) = 18.1$ and 17.4 for [DL]-[**2**H]$^+$[I]$^-$ and [*meso*]-[**2**H]$^+$[I]$^-$, respectively) might be taken to indicate that the hydrogen bonding is similar in both diastereomers and can be categorised, according to the model of Forsén et al.,[18] as strong with a double minimum on the potential surface, that is not a *low-barrier hydrogen bond*. However, isotopic fractionation factors and primary isotope effects on chemical shift are often interpreted without regard for other intramolecular vibrations or solvation which will affect differences in H/D zero-point energy differences on the hydrogen-bond potential surface. Recent calculations from Messina et al. indicate that in a rigid "A–H···B" model in which internal vibrations in A and B are ignored, low-frequency intramolecular vibration (ca. 200 cm^{-1}) coupled to the hydrogen-bond coordinate can substantially reduce the calculated fractionation factor.[19] Since a low-fractionation factor is often taken as being indicative of a low-barrier hydrogen bond, these calculations indicate that such conclusions must, in some cases, be drawn cautiously. Similarly, recent reports from Perrin and Nielson[20] demonstrate that primary isotope shifts in O–H–O hydrogen-bonded systems (e.g. maleate) are highly solvent dependent (varying from positive to negative) and this again emphasises the caution that must be exercised in interpretation of this data. Perrin and Nielson recommended the use of secondary isotope shifts (e.g. ^{18}O) since these were found to be reasonably consistent in sign and magnitude in a range of solvents.

The stereodynamics of [2H]$^+$: In light of the IR and NMR data for [**2**H]$^+$ being indicative of strong hydrogen bonding and the close structural similarity of [**2**H]$^+$ to [**1a**H]$^+$, the surprising stereolability of [**2**H]$^+$ seemed an important phenomenon to study in more detail. Careful measurement of the stereodynamics would lead to informative data regarding the enthalpic and entropic contributions to the activation parameters for stereomutation of [**2**H]$^+$. Unlike our earlier work with **2**,[17b] the stereodynamics of [**2**H]$^+$ could not be measured by NMR line-shape analysis due to the activation barrier to conformation exchange in [**2**H]$^+$ requiring temperatures at which decomposition occurs. We thus turned to selective magnetisation-transfer experiments using ^{13}C NMR spectroscopy (rather than ^{1}H NMR spectroscopy so as to exploit the larger T_1 values) and [^{13}C–**2**H]$^+$[I]$^-$[17] in which a single methyl group is 99% ^{13}C-labelled so as to gain an approximately 50-fold increase in sensitivity over the unlabelled material. Magnetisation-transfer[21] to the $^{13}CH_3$ of [*meso*]-[^{13}C–**2**H]$^+$[I]$^-$ (0.31M in [D$_7$]DMF)[22] on selective inversion of the $^{13}CH_3$ signal of [DL]-[^{13}C-**2**H]$^+$[I]$^-$ by a 1-2-1 pulse train was observed at 100, 105, 110, 115 and 120 °C with delay times (D_2) spanning a range of 2 to 7000 ms. First-order rate constants τ_1 ($= T_1^{-1}$) for the relaxation of inverted [*meso*]- and [DL]-[^{13}C–**2**H]$^+$[I]$^-$ between 100–120 °C were predicted by extrapolation of linear plots of $\ln(\tau_1/T)$ versus $(1/T)$ determined between 25 and 105 °C (Figure 1; upper graph). Equilibrium populations were predicted by extrapolation of a van't Hoff plot ($\ln K_{eq}$ versus $1/T$) (Figure 1; lower graph).

With τ_1 and K_{eq} ($= k_{DL\rightarrow meso}/k_{meso\rightarrow DL}$) values for each temperature, rate constants for interconversion were then obtained

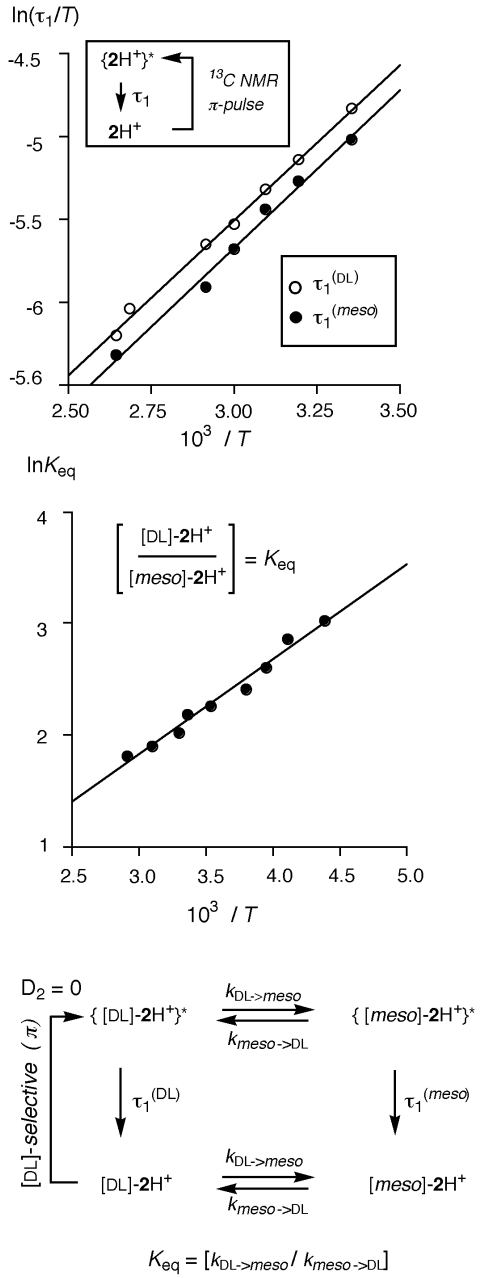

Figure 1. Top: Eyring type analysis of the variation of ^{13}C NMR (125 MHz) relaxation rate, τ_1 ($= T_1^{-1}$) of the ^{13}C-labelled methyl group of [DL]-[^{13}C-**2**H]$^+$[I]$^-$ and [*meso*]-[^{13}C-**2**H]$^+$[I]$^-$ in [D$_7$]DMF between 25 and 70 °C. Centre: van't Hoff type analysis of the equilibrium populations of [DL]-[^{13}C-**2**H]$^+$[I]$^-$ and [*meso*]-[^{13}C-**2**H]$^+$[I]$^-$ in [D$_7$]DMF between –45 and +70 °C (by ^{13}C NMR, 100 MHz).

 © WILEY-VCH Verlag GmbH, D-69451 Weinheim, 2000 0947-6539/00/0624-4453 $ 17.50+.50/0

by iteration of $k_{DL\text{Æ}meso}$ in the kinetic model outlined at the bottom of Figure 1 until a best fit of predicted population (%) of *unmagnetised* [*meso*] diastereomer was obtained (Figure 2 and Table 1).[23]

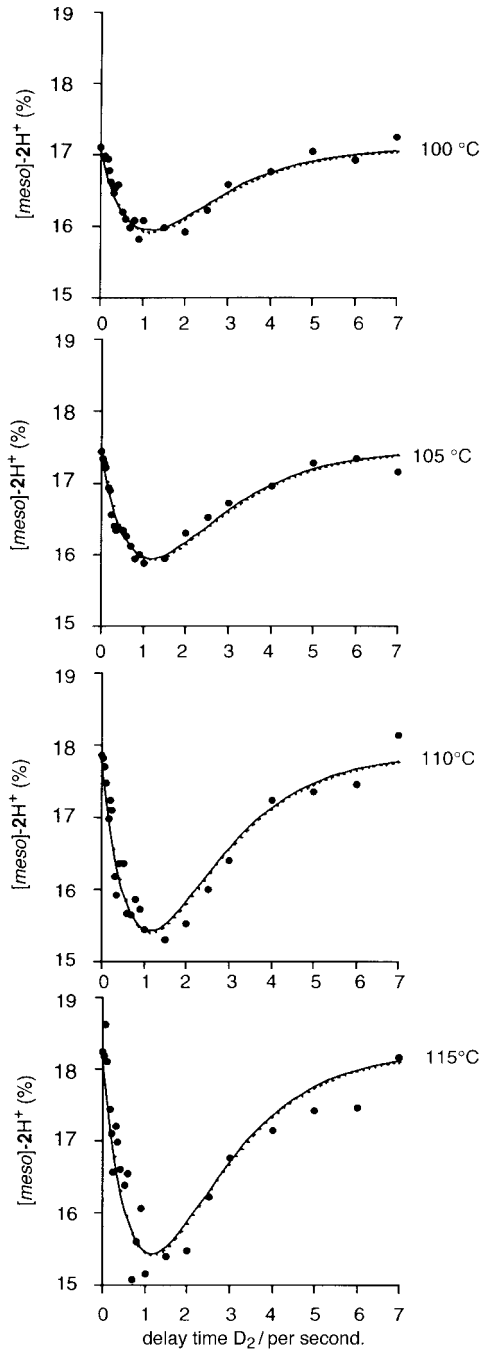

Figure 2. ^{13}C NMR, 125 MHz magnetisation transfer experiments (see model at bottom of Figure 1) in which the intensity of the peak corresponding to the *unmagnetised* (0° phase) ^{13}C-labelled Me group in [*meso*]-[^{13}C-**2**H]$^+$[I]$^-$ is monitored after selective magnetisation (180° phase) of the ^{13}C-labelled Me group in [DL]-[^{13}C-**2**H]$^+$[I]$^-$ (total concentration 0.0309 M in [D_7]DMF).

To obtain values for enthalpy and entropy of activation with a reasonable level of confidence, the rates of interconversion at a fairly wide temperature range must be studied. Below 100 °C the rates were not sufficient to attain reasonable magnetisation transfer before relaxation of the $^{13}CH_3$ signal of [DL]-[^{13}C-**2**H]$^+$[I]$^-$, whilst above 120 °C significant decomposition began to occur during the run time. We therefore attempted to study the stereodynamics by measuring the rate of *approach* to equilibrium rather than rate of interconversion *at* equilibrium. We first tested the feasibility of dissolution of single crystals (which we have shown by X-ray crystallography to be exclusively [DL]-[**2**H]$^+$[I]$^-$)[17a] at a temperature below that at which rapid equilibration occurs. Although carefully powdered single crystals[24] were scarcely soluble in common deuterated solvents at low temperature, [D_7]DMF proved sufficiently polar and we were able to dissolve powdered single crystals at −50 °C within about 5 min with only a slight degree of equilibration (ca. 98:2 [DL]/[*meso*]). In the ^1H NMR spectrum, the only signals displaying suitable dispersion ($\Delta\delta$) between [DL] and [*meso*] were those due to $^+N{-}H\cdots N$ (at $\delta = 18.86$ and 19.47, respectively) but the broad nature of these signals resulted in poor signal-to-noise ratios. We therefore resorted to studying samples of [DL]-[^{13}C–**2**H]$^+$[I]$^-$ by ^{13}C NMR spectroscopy. However, as was predicted by the earlier population versus temperature studies (Figure 1, lower graph) the 2% change between about 98:2 (single-crystal dissolution) and about 96:4 (equilibrium population at −50 °C) resulted in very poor kinetic data.

An alternative approach lay in attaining a static equilibrium enriched in the [*meso*] isomer, thereby allowing the decay, rather than growth, of [*meso*] to be followed on approach to equilibrium. Flash cooling (−78 °C, CO_2/acetone bath) of 130 °C (oil bath) samples of [^{13}C–**2**H]$^+$[I]$^-$ in [D_7]DMF in an NMR tube ($-\Delta T \geq 200$ °C, ≤5 s) reproducibly gave a static (m.p. [D_7]DMF ca. −62 °C) nonequilibrium population of about 81:19 [DL]/[*meso*]—see arrow connecting filled circles in Figure 3.

Samples were then allowed to rapidly melt in the probe of a 400 MHz (^1H) NMR spectrometer at a given temperature and the rates of relaxation to the equilibrium population (−50 °C

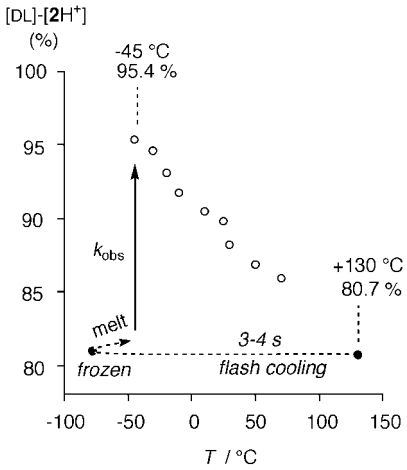

Figure 3. Variation of equilibrium populations of [DL]-[^{13}C-**2**H]$^+$[I]$^-$ and [*meso*]-[^{13}C-**2**H]$^+$[I]$^-$ in [D_7]DMF (as % [DL]-) with temperature (open circles). Filled circles: start (+130 °C) and end (−78 °C) points for flash cooling ($-\delta T/\delta t \geq 208$ °C in 5 s) of dynamic equilibrium population (ca. 80.5:19.5 [DL/*meso*]) to static non-equilibrium population (ca. 81.5:18.5) below the freezing-point of the solvent (ca. −62 °C) used for monitoring kinetics of equilibration by ^{13}C NMR spectroscopy between −53 and −36 °C, see Figure 4.

© WILEY-VCH Verlag GmbH, D-69451 Weinheim, 2000
0947-6539/00/0624-4454 $ 17.50+.50/0 *Chem. Eur. J.* **2000**, *6*, No. 24

ca. 96:4 [DL]/[*meso*]) were monitored by $^{13}C\{^1H\}$ NMR spectroscopy ($\Delta\delta = CH_3$ ca. 0.6). Use of ^{13}C-labelled [^{13}C-**2**H]$^+$[I]$^-$ allowed spectra to be acquired rapidly and with excellent signal-to-noise ratios. The data thus obtained from four runs (at -53, -46 , $-41\,^\circ C$ and $-36\,^\circ C$) are given in Figure 4.

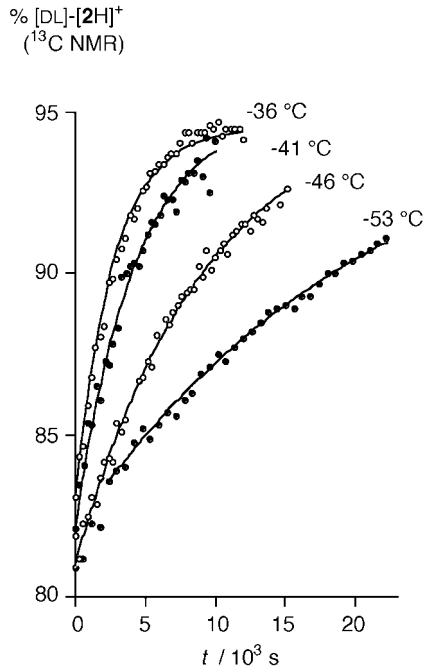

Figure 4. Data points: rates of attainment of equilibrium populations of [DL]-[^{13}C-**2**H]$^+$[I]$^-$ and [*meso*]-[^{13}C-**2**H]$^+$[I]$^-$ in [D_7]DMF at -53, -46, -41 and $-36\,^\circ C$ as determined by ^{13}C NMR spectroscopy from static non-equilibrium populations (for generation see Figure 3). Solid lines: kinetic models generated by a first-order model using equilibrium populations derived from van't Hoff analysis (Figure 1).

Knowing the final equilibrium constants (see Figure 1), we were readily able to fit the data to a simple reversible first-order kinetic model from which rate constants $k_{DL\rightarrow meso}$ and $k_{meso\rightarrow DL}$ could be extracted (Table 1).

Combined with the rates obtained from magnetisation transfer at higher temperature (vide supra) an Eyring analysis (Figure 5) over a temperature range of 172 °C allowed reliable

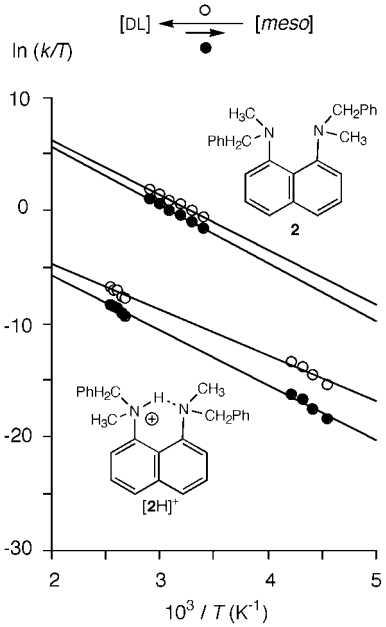

Figure 5. Eyring analysis of rates of interconversion of [DL] (filled circles) and [*meso*] (open circles) diastereomers of [**2**H]$^+$[I]$^-$ (lower pair of lines, data by ^{13}C NMR magnetisation transfer and first-order equilibrium attainment in [D_7]DMF) and for comparison **2** (upper pair of lines, data by ^{13}C NMR line-shape analysis in [D_7]DMF—data from reference [174b]). Error weighted linear regression for conversion of [DL]- to [*meso*]-[**2**H]$^+$[I]$^-$, $\ln(k/T) = 4.1(\pm 0.3) - 4928(\pm 76)/T$, and for [*meso*]- to [DL]-, $\ln(k/T) = 3.5(\pm 0.4) - 4084(\pm 100)/T$.

Table 1. First-order rate constants for the interconversion of [DL]-/[*meso*]-[**2**H]$^+$[I]$^-$ and [DL]-/[*meso*]-**2** in [D_7]DMF at various temperatures as determined by ^{13}C NMR spectroscopy of methyl [$^{13}C_1$]-labelled compounds.

Entry	T [K]	Method[a]	Compound	$k_{DL\rightarrow meso}$ [s^{-1}] ($\pm$error)	$k_{meso\rightarrow DL}$ [s^{-1}] ($\pm$error)	$\Delta G^{\ddagger}_{DL}$[d] [kcal mol^{-1}] ($\pm$error)	$\Delta G^{\ddagger}_{meso}$[d] [kcal mol^{-1}] ($\pm$error)
1	219.9	A	[**2**H]$^+$[I]$^-$	$2.1(0.1)\times10^{-6}$	$48.4(2)\times10^{-6}$	18.4(0.1)	17.1(0.2)
2	226.9	A	[**2**H]$^+$[I]$^-$	$5.3(0.1)\times10^{-6}$	$107(14)\times10^{-6}$	18.6(0.1)	17.3(0.2)
3	232.0	A	[**2**H]$^+$[I]$^-$	$12.2(0.8)\times10^{-6}$	$233(15)\times10^{-6}$	18.8(0.1)	17.3(0.1)
4	237.1	A	[**2**H]$^+$[I]$^-$	$20.2(2)\times10^{-6}$	$348(22)\times10^{-6}$	18.9(0.1)	17.6(0.1)
5	372.5	B	[**2**H]$^+$[I]$^-$	$3.3(0.3)\times10^{-2}$	$16.0(1.5)\times10^{-2}$	24.5(0.1)	23.3(0.1)
6	377.5	B	[**2**H]$^+$[I]$^-$	$4.2(0.3)\times10^{-2}$	$19.7(1.4)\times10^{-2}$	24.6(0.1)	23.5(0.2)
7	382.5	B	[**2**H]$^+$[I]$^-$	$7.1(0.5)\times10^{-2}$	$32.6(2.3)\times10^{-2}$	24.6(0.1)	23.4(0.1)
8	387.5	B	[**2**H]$^+$[I]$^-$	$8.0(0.6)\times10^{-2}$	$35.9(2.7)\times10^{-2}$	24.8(0.1)	23.7(0.2)
9	392.5	B	[**2**H]$^+$[I]$^-$	$9.7(1.7)\times10^{-2}$	$42.4(7.4)\times10^{-2}$	25.0(0.2)	23.8(0.2)
10	293.7	C	**2**	58 (3)	158 (9)	14.8(0.2)	14.2(0.1)
11	303.2	C	**2**	111(4)	294 (11)	14.9(0.2)	14.3(0.2)
12	312.9	C	**2**	204(7)	525(18)	15.0(0.2)	14.4(0.1)
13	323.1	C	**2**	301(14)	754 (35)	15.3(0.1)	14.7(0.1)
14	333.2	C	**2**	566(11)	1386 (27)	15.4(0.1)	14.8(0.1)
15	343.3	C	**2**	884(13)	2119 (31)	15.6(0.1)	15.0(0.1)

[a] Method A: attainment of equilibrium population from a static non-equilibrium population (for generation see Figure 3) as determined by analysis of ^{13}C NMR signal of labelled methyl group. Method B: magnetisation transfer from ^{13}C NMR signal of labelled methyl group of [DL]-[^{13}C-**2**H]$^+$[I]$^-$ to [*meso*]-[^{13}C-**2**H]$^+$[I]$^-$, spin polarisation (180 °) of [DL]-[^{13}C-**2**H]$^+$[I]$^-$ generated by a 1-2-1 pulse train (see Figure 2). Method C: Variable temperature dynamic ^{13}C NMR of labelled methyl group; data taken from reference [17b]. [b] Rate constants generated by iterative fitting of a kinetic model to time versus relative concentration (method A), delay time versus peak height (method B), full band shape analysis (method C).[c] Equilibrium populations predicted by van't Hoff analyses (for [^{13}C-**2**H]$^+$[I]$^-$ see Figure 1). [d] Calculated from $\Delta G^{\ddagger} = RT[\ln h/k_B - \ln k/T]$.

extraction of thermodynamic parameters (Table 2). Of note is the parallel relationship between linear regression of kinetic data from protonated [**2**H]$^+$ (lower pair of lines) versus non-protonated **2** (upper pair of lines) forms, indicative of very similar *enthalpic* barriers to interconversion of diastereoisomers.

Table 2. Activation parameters for the interconversion of methyl [$^{13}C_1$]-labelled [DL]-/[*meso*]-[**2**H]$^+$[I]$^-$ and [DL]-/[*meso*]-**2** in [D_7]DMF at 298 K as determined by error-weighted linear regression of Eyring analyses[a,b,c,d] (see Figure 5, data from Table 1).

Entry	Compound	$\Delta G^{\ddagger}_{298}$[d] [kcal mol^{-1}] (± error)	$\Delta H^{\ddagger}_{298}$ [kcal mol^{-1}] (± error)	$\Delta S^{\ddagger}_{298}$[d] [J K^{-1} mol^{-1}] (± error)	$T\Delta S^{\ddagger}_{298}$[d] [kcal mol^{-1}] (± error)
1	[DL]-[**2**H]$^+$[I]$^-$ [a]	21.4 (0.5)	9.8 (0.2)	− 163 (4)	− 11.6 (0.3)
2	[*meso*]-[**2**H]$^+$[I]$^-$ [b]	20.1 (0.5)	8.1 (0.2)	− 169 (4)	− 12.0 (0.3)
3	[DL]-**2**[c]	14.8 (0.4)	10.0 (0.2)	− 67 (3)	− 4.8 (0.2)
4	[*meso*]-**2**[d]	14.2 (0.4)	9.5 (0.2)	− 66 (3)	− 4.7 (0.2)

[a] $\ln(k/T) = 4.1(\pm 0.3) - 4928(\pm 76)/T$. [b] $\ln(k/T) = 3.5(\pm 0.4) - 4084(\pm 100)/T$. [c] $\ln(k/T) = 15.7\ (\pm 0.4) - 5057(\pm 117)/T$. [d] $\ln(k/T) = 15.8(\pm 0.4) - 4798(\pm 116)/T$.

Mechanisms for interconversion of diastereoisomers of [2H]$^+$: Although [**2**H]$^+$[I$^-$] was analytically pure and by NMR spectroscopy there was no trace of any impurity, the first mechanism for diastereoisomer interconversion that should be considered is one in which trace quantities of [**2**H]$^+$[I$^-$] are reversibly deprotonated to afford **2** (which has a lower barrier towards diastereoisomer interconversion).[17b] Although the steric bulk of **2** would no doubt make its action as a base on another molecule of [**2**H]$^+$[I$^-$] kinetically negligible, a catalytic quantity of water could transport protons between [**2**H]$^+$[I$^-$] and **2** and therefore accelerate the apparent stereodynamic processes of [**2**H]$^+$[I$^-$]. However, addition of traces of water to organic solutions of [**2**H]$^+$[I$^-$] resulted in immediate precipitation of the salt. This result, when considered alongside our earlier observations[17b] on the reaction of **3** with CD_3I, suggests that water is not responsible.[25] Another indirect process that may be considered is one in which **3** is reversibly generated by iododealkylation (the energy barrier to automerisation of **3** is substantially lower than 14 kcal mol^{-1} at 298 K).[17b] Such processes are well documented, for example the spontaneous resolution on crystallisation of ammonium salt **5** arises by automerisation occurring through nucleophilic attack of the iodide counterion on the allyl group.[26] The resulting tertiary amine may invert prior to re-allylation by allyl iodide. To test for a similar mechanism with [**2**H]$^+$[I$^-$] we added three equivalents of $^{13}CH_3I$ to an 0.07 M solution of [**2**H]$^+$[I$^-$] in CD_2Cl_2. After two days at ambient temperature there was no evidence for any ^{13}C-label incorporation in [**2**H]$^+$[I$^-$] and thus no evidence for reversal to **3**. Similarly, exchange of $^{13}CH_3I$ with benzyl iodide would be expected if iodide was attacking the benzyl groups[27b] to generate **4** and, again, this is not observed.

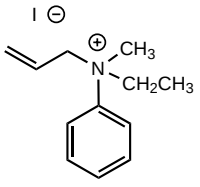

(±)-**5**

We are thus left to consider the mechanism for *direct*[28] interconversion of the diastereoisomers of [**2**H]$^+$[I$^-$]. The kinetics of interconversion of [DL] and [*meso*] isomers of [**2**H]$^+$I$^-$ (vide supra) follow a first-order (or pseudo-first-order) dependence on [**2**H]$^+$[I]$^-$ and the most simple unimolecular mechanism would be one in which hydrogen bond fission is followed by or accompanied by correlated inversion–rotation at the nonprotonated nitrogen centre. This mechanism is consistent with the extensive work of Hibbert et al.,[29] on the proton-transfer from **7**H$^+$.[8] It should be noted that **7** is about 10^4-fold more basic than **1a** (and likely **2**).[27]

Hibbert et al., studied in detail the kinetics of the equilibria between protonated and non-protonated species (**7** → **7**H$^+$; **7**H$^+$ → **7**) measured by using a fast temperature-jump (ΔT ca. +4 °C, 2–3 μs) to attain a non-equilibrium distribution and following relaxation to the new equilibrium population by UV. The mechanism proposed for equilibrium between [**7**H]$^+$ and **7** is one in which proton transfer to base occurs *via* the non-hydrogen bonded intermediate [*nonHB*-**7**H]$^+$ as shown in Scheme 2. Good evidence for this pre-equilibrium, for

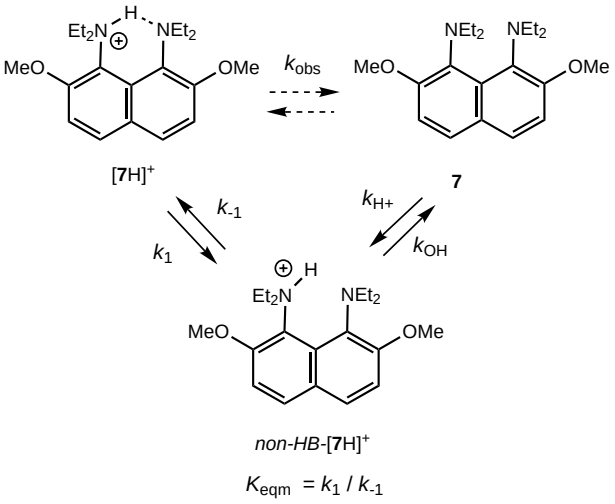

Scheme 2. The Hibbert model for the interconversion of [**7**H]$^+$ and **7** by a two-step process involving hydrogen bond fission to give a low equilibrium population (K_1) of *non-HB*-[**7**H]$^+$, followed by deprotonation by base (k_2).

which K_{eqm} is roughly equal to 10^{-6}, comes from positively displaced biphasic Brønsted plots.[29, 8b] In effect, by studying the *stereodynamics* of [**2**H]$^+$ we have performed a kinetic analysis of the first stage of the mechanism proposed by Hibbert et al. for the deprotonation of protonated proton sponges. As such, the mechanism for [**7**H]$^+$ can be contracted for [**2**H]$^+$ so that only the unimolecular processes are considered (Scheme 3). Now, instead of using a bimolecular reaction (with OH$^-$) as a kinetic probe (Scheme 2), we can use the inversion of nitrogen configuration (k_2 and k_{-2}) since this unimolecular process can only occur when the hydrogen bond is broken (k_1, Scheme 3). One might describe this situation as an intramolecular equivalent of the Saunders and Yamada experiment with *N*-methyldibenzylamine.[30]

To use this model, we needed to calibrate the k_2 "clock", that is, the energetics of inversion of nitrogen configuration. Consequently, we attempted (unsuccessfully) to synthesise

© WILEY-VCH Verlag GmbH, D-69451 Weinheim, 2000
0947-6539/00/0624-4456 $ 17.50+.50/0 *Chem. Eur. J.* **2000**, *6*, No. 24

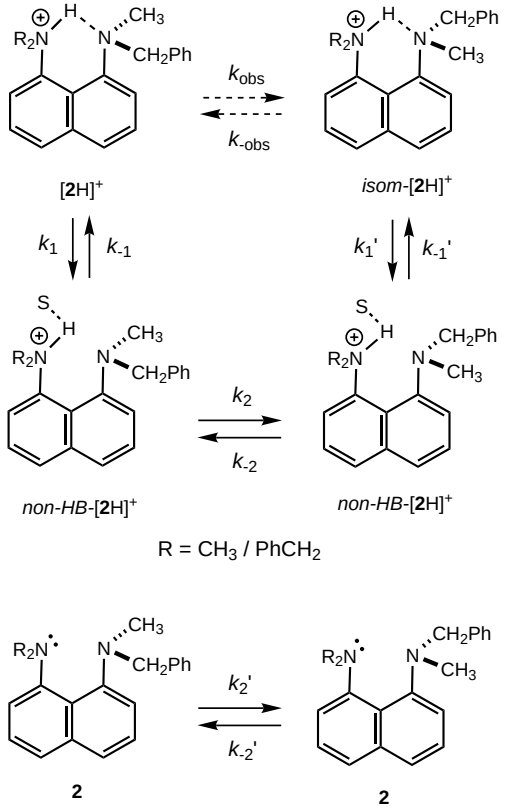

Scheme 3. Model for the interconversion of [DL]-[**2**H$^+$] and [*meso*]-[**2**H$^+$] by a two-step process involving solvent-assisted (S = [D$_7$]DMF) hydrogen bond fission (k_1) to give *non-HB*-[**2**H]$^+$, followed by rotation-inversion (k_2) and then hydrogen bond formation. The stereodynamics of **2** may possibly be used as a crude model for the stereodynamics of the equilibrium population (K_1) of *non-HB*-[**2**H]$^+$.

isosteric monoamine **6** in which the passage of a methyl group through the space between the C and N is blocked by a proton (C–H) but there is no ammonium hydrogen with which the free amine may hydrogen bond.[31] Nonetheless, we have already studied the energetics of the stereodynamics of the free-base (1,8-bis-(*N*-benzyl-*N*-methylamino)naphthalene **2**) in some detail,[17b] see lower process (k_2' and k_{-2}') in Scheme 3, and this may serve as a useful model for [*nonHB*-**2**H]$^+$. The energetics for stereodynamics of **2** and [**2**H]$^+$I$^-$ are compared (at 298 K) in Figure 6.

(±)-**6**

Despite the higher activation barrier ($\Delta G^{\neq}$) for diastereomer interconversion of [**2**H]$^+$, the enthalpy of activation ($\Delta H^{\neq}$) is very similar to that found for rotation-inversion of a non-protonated nitrogen centre in **2**[17b] (Figure 6). The increased barrier ($\Delta\Delta G^{\neq}_{298}$ = ca. 5.9 and 6.6 kcal mol^{-1}) is a consequence of the much larger entropic contribution ($T\Delta S^{\neq}$ = 12.0 (±0.3) and 11.6 (±0.3) kcal mol^{-1}) to the global barrier (k_{obs} and k_{-obs}) to diastereomer interconversion of [**2**H]$^+$ in both directions.[32] It therefore seems reasonable that the solvent [D$_7$]DMF is actively involved in the exchange process and must become significantly more ordered on approach to one or more transition states. There is no reason to expect that

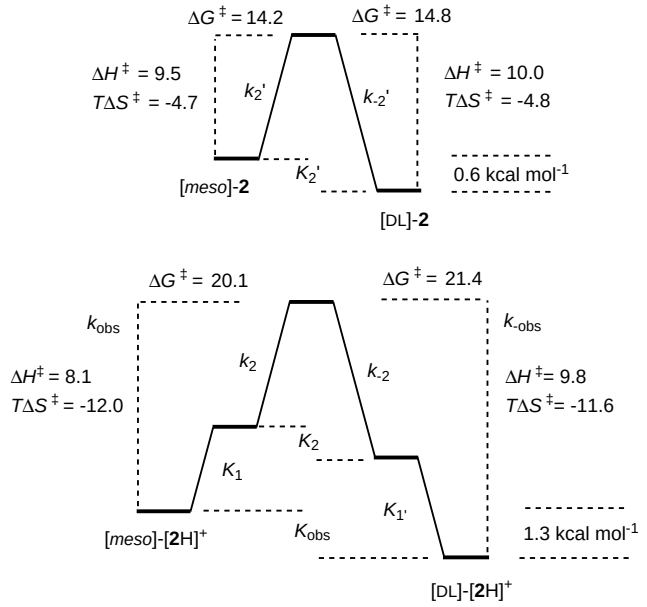

Figure 6. Energy map (kcal mol^{-1}) for stereodynamics of [DL]- and [*meso*]-[**2**H$^+$] (lower section) and [DL]- and [*meso*]-**2** (upper section). The thermodynamic parameters for **2** (see k_2' and k_{-2}' in Scheme 3) may possibly be used as a crude model for the stereodynamics of *non-HB*-[**2**H]$^+$ (k_2 and k_{-2} in Scheme 3) and thereby gain access to thermodynamic information regarding K_1 in Scheme 3. Note. The vertical dimension (E) and horizontal dimension (reaction coordinate) are not to scale and the lines connecting states are merely drawn as an aid for the eye.

the situation in [**1a**H]$^+$ (which lacks *N*-chirality and cannot be analysed analogously by NMR) will be any different. A likely role for the solvent is hydrogen bonding of the carbonyl oxygen of the DMF with the ammonium ion in [*nonHB*-**2**H]$^+$. Indeed, Hibbert has suggested hydrogen bonding of sulphoxide to [*nonHB*-**7**H]$^+$ as a possible reason for the DMSO acceleration of equilibration of **7** and [**7**H]$^+$ in aqueous media.[33] Our interpretation of these results is that since protonation of one amine centre (i.e., **2** → [**2**H]$^+$) has little *net* effect on the *enthalpy* of activation ($\Delta H^{\neq}$) for stereodynamics at the non-protonated centre, the intramolecular hydrogen bond in [**2**H]$^+$ is roughly equal in enthalpic strength (ΔH) with that made with the solvent ([D$_7$]DMF) in the non-hydrogen-bonded intermediate [*non*HB-**2**H$^+$].

X-ray crystallographic studies of **2**[17b] and [**2**H]$^+$[17a] show severe distortion of the planarity of the naphthalene ring in free-base **2** (deviation from ideal planarity is some 0.3 Å) but not at all in the protonated form [**2**H]$^+$. However, NMR studies of the *free-base* **3** indicate that strain analogous to that in **2** is relieved by trigonalisation of the NH centre and hydrogen bonding with the tetrahedral tertiary amine centre at the peri position.[17b] This is, of course, not feasible in **2**. The hydrogen bonding in [**2**H]$^+$ (and thus [**1a**H]$^+$) may be considered as predominantly an entropically driven process, without any unusual enthalpic strength. It is more favourable for the ammonium salt to be hydrogen-bonded *intramolecularly* than intermolecularly (with solvent) since the latter costs order (entropy). Even so, the N–N distance in both [**2**H]$^+$ and [**1a**H]$^+$ (ca. 2.65 and 2.60 Å, respectively) indicate that the hydrogen bond is under compression and thus not ideal.[34] Since the hydrogen bonding in [**1b**H]$^+$ is not expected to be

significantly different from that in [**1a**H]$^+$,[9] the 10^6-fold higher basicity of the archetypal proton sponge 1,8-bis-(*N*,*N*-dimethylamino)naphthalene **1a** as compared with the desmethyl analogue 1,8-*N*,*N*,*N*′-trimethylamino-1,8-diaminonaphthalene **1b** must also be ascribed predominantly to *destabilisation* of the free-base (**1a**) and, in analogy to **2**,[17b] stabilisation of free-base **1b** through intramolecular hydrogen bonding.

Conclusion

The readily prepared *N*,*N*-chiral proton sponge **2** and its salt [**2**H]$^+$ can exist as two diastereomers, (chiral [DL]- and achiral [*meso*]-) whose stereochemical identities in solution (NMR) and structures in the solid state (X-ray) have already been established. Physical data (NMR, IR) for the protonated form [**2**H]$^+$, which is structurally quite similar to the archetypal protonated proton sponge [**1a**H]$^+$, would suggest that the hydrogen bond is a *low-barrier hydrogen bond* . This, in turn, has led some to suggest that the hydrogen bond in protonated first generation proton sponges must therefore be "short and strong". Indeed, a value of about 17 kcal mol^{-1} has been suggested for [**1a**H]$^+$.[7a] However, contrary to expectation, pure [DL]-[**2**H]$^+$ was found to be stereolabile in solution at ambient temperatures with the equilibrium population (which favours [DL]-[**2**H]$^+$ isomer over the [*meso*]-[**2**H]$^+$ isomer) being reached within minutes at 21 °C.

The kinetics of the stereodynamic processes that effect interconversion of the [DL]- and [*meso*]-forms of [**2**H]$^+$ (k_{obs} and k_{-obs}) have been studied by NMR spectroscopy using rapid temperature drop methods (+130 °C → −78 °C) and magnetisation transfer. Eyring analysis (over a 170 °C temperature range) allows comparison of activation parameters with the analogous processes occurring in the free base **2**. For the protonated form, the *total* activation barrier from ground state [*meso*]-[**2**H]$^+$[I]$^-$ to the transition state effecting interconversion with [DL]-[**2**H]$^+$[I]$^-$ is about 20.1 (±0.5) kcal mol^{-1} at 298 K and about 5.9 kcal mol^{-1} higher than for **2**. Similarly, for [DL]-[**2**H]$^+$[I]$^-$ the barrier is 21.4 (±0.5) kcal mol^{-1} at 297 K (6.6 kcal mol^{-1} higher than for **2**). However, in both directions, the increased barrier (relative to **2**) is almost completely caused by an increased *entropic* ($T\Delta S^{\neq}$ = 12.0 (±0.3) and 11.6 (±0.3) kcal mol^{-1}) and not *enthalpic* barrier. Consequently, a pseudo-unimolecular mechanism in which hydrogen bond fission (K_1 ca. 10^{-5})[35] is followed by or accompanied by hydrogen-bonding with the solvent ([D$_7$]DMF) and inversion-rotation of the non-protonated nitrogen centre (Scheme 3) suggests that the enthalpic strength of the hydrogen bond in both [DL]-[**2**H]$^+$ and [*meso*]-[**2**H]$^+$ is no greater than the intermolecular one formed with the solvent ([D$_7$]DMF). This value will not be much different from that in [**1a**H]$^+$, the protonated form of the archetypal proton sponge. The normality of the hydrogen bond is consistent with the values estimated by Hibbert et al. for [**7**H]$^+$[8, 36] and suggested by Guthrie for [**1a**H]$^+$.[7b] The extraordinary basicity of the first-generation proton sponges is therefore largely due to the relief of steric strain on protonation and not due to the accompanying formation of an intramolecular hydrogen bond, which whilst definitely present and possibly a "low-barrier hydrogen bond" is not a "short – strong hydrogen bond".

Experimental Section

General: All manipulations and reactions were carried out under an N_2 or Ar atmosphere using standard Schlenk techniques. The preparation of [[$^{13}C_1$]-**2**H]$^+$[I]$^-$ (99 % $^{13}CH_3$) and *N*(benzyl)-*N*′(benzylmethyl)-1,8-diaminonaphthalene (**3**) have been reported in full elsewhere.[17b] [D$_7$]DMF was purchased from Goss Scientific Ltd. D_2O was purchased from Fluorochem. NMR experiments were performed in 5 mm NMR tubes (Wilmad) on JEOL GX400 and JEOL Alpha 500 Instruments fitted with variable temperature probes. Temperatures were measured by a thermocouple (located within the probe head) which was calibrated by use of a "methanol thermometer".[37] The values measured during NMR experiments were corrected accordingly and are estimated to be accurate to $\leq \pm 0.8$ K.

Deuterium iodide salt of 1,8-bis-(*N*-benzyl-*N*-methylamino)naphthalene [2D]$^+$[I]$^-$: *N*-(benzyl)-*N*′-(benzylmethyl)-1,8-diaminonaphthalene (**3**) (146 mg, 0.13 mmol) was dissolved in CH_2Cl_2 (ca. 3 mL) giving a light brown solution. D_2O (ca. 1 mL) was added and the solution was made slightly basic by addition of LiOMe (ca. 5 mg). The two phases where agitated to promote exchange. The D_2O layer was removed and the process repeated a further two times. The organic layer was then dried over CaH_2 (ca. 3 mg) and the volatiles removed in vacuo giving [D$_1$]**3** as a light brown oil. This was converted to [**2D**]$^+$[I]$^-$ without further purification by dissolution in methyl iodide (ca. 1 mL) in an ampoule resulting in an dark orange solution. The ampoule was sealed and the solution was left a room temperature for two days during which crystallisation occurred at the upper surface of the solution. The excess methyl iodide was decanted. The pale yellow crystals were washed with a small amount of methyl iodide (ca. 0.1 mL) and dried *in vacuo* to give [**2D**]$^+$[I]$^-$ as pale yellow crystals. ^{2}H NMR (CH_2Cl_2, 60 MHz, 28 °C, CD_2Cl_2) [DL]-[**2D**]$^+$[I]$^-$ (s, 17.3, ND); [*meso*]-[**2D**]$^+$[I]$^-$ (s, 16.6, ND). ^{1}H NMR analysis (integration of CH_3 against N–H) indicated a ^{2}H-incorporation of 64 %.

NMR experiments

Rapid temperature drop: ^{13}C{^{1}H} NMR experiments were performed in 5 mm NMR tubes at 100 MHz using 99 % ^{13}C [$^{13}C_1$-**2**H]$^+$[I]$^-$ (15 mg of a powdered sample was dissolved in 1.0 g [D$_7$]DMF). Samples were heated by immersion of the lower half of the tube in an oil bath at 130 °C for 30 s. The tube was then removed from the oil bath and with vigorous agitation the lower half plunged into a dry-ice/acetone bath (liquid nitrogen was much less effective at *rapid* cooling) until the solution became very viscous and eventually froze. Tests performed with a thermocouple immersed into 1.0 g [D$_7$]DMF in a 5 mm tube indicated that a temperature drop from 130 °C to −70 °C was achieved in less than 5 s, even though complete freezing (m.p. [D$_7$]DMF ca. −61 °C) took some minutes. Rates of approach to equilibrium were then measured at −53, −46, −41 and −36 °C (using 30 mg [$^{13}C_1$-**2**H]$^+$[I]$^-$ instead of 15 mg) as follows. After shimming the NMR spectrometer on an identical ("dummy") sample at the desired temperature, the probe was cooled to −60 °C and the dummy sample exchanged rapidly with the frozen non-equilibrium sample (at −78 °C). The probe was then rapidly returned to the desired temperature by which point the sample had melted and the instrument locked onto the ^{2}H signal from the solvent. For the runs at −53, −46 and −41 °C, an array of n × 256 pulse-sequences (each sequence of duration 2 s with 0.655 s accumulation time and each set of 256 pulses being started at 10 min intervals) were performed. With the run at −36 °C, an array of identical n × 128 pulses were run at 5 min intervals. Each FID was Fourier transformed (after application of a Gausssian Window, BF −0.6 Hz, GF = 3.0 Hz) and phased manually. Integration of the signals at δ = 53.0 and 53.7 was then used to establish the ratio of [DL] versus [*meso*] respectively.

Magnetisation transfer: ^{13}C{^{1}H} NMR experiments were performed at 125 MHz using 99 % ^{13}C [$^{13}C_1$-**2**H]$^+$[I]$^-$ (15 mg in 1.0 g [D$_7$]DMF). Longitudinal relaxation rates ($T_1 = 1/\tau_1$) were measured at 25, 40, 50, 60, 70, 99.5 and 105 °C by linear regression of peak intensities from standard inversion – recovery experiments.[38] The Eyring relationships found for [DL] and [*meso*] isomers were $(\ln\tau_1/T) = 1870/T\ (\pm 51) - 11.1(\pm 0.15)$ (r^2 =

© WILEY-VCH Verlag GmbH, D-69451 Weinheim, 2000
0947-6539/00/0624-4458 $ 17.50+.50/0 *Chem. Eur. J.* **2000**, *6*, No. 24

0.996) and 1897 (±99) −11.4 (±0.3) ($r^2 = 0.989$), respectively. Magnetisation transfer was performed at 100, 105, 110, 115 and 120 °C as follows: After determination of the 90 degree pulse width (15.5 μs), the spectral window was adjusted so that the methyl signal of the major (DL) diastereomer at $\delta = 53.03$ was "on resonance". A [(π/4)-D_1-(π/2)-D_1-(π/4)-D_2-(π/2)-accumulate] pulse sequence was applied, where: $D_1 = 1/2\Delta\tilde{\nu} =$ 6.2 ms (thereby inverting the signal of the [DL] isomer with no *net* inversion of the minor (*meso*) isomer at 53.66 ppm) and D_2 = variable delay time (0.002, 0.05, 0.1, 0.15, 0.2, 0.25, 0.3, 0.35, 0.4, 0.5, 0.6, 0.7, 0.8, 0.9, 1, 1.5, 2, 2.5, 3, 4, 5, 6 and 7 s). A series of five ($D_2 = 2$ ms) control peaks were inserted into the D_2-array of variable delay time. Very slow, zero-order, decomposition (up to ca. 10 % at 120 °C over the total run time) of $[\mathbf{2H}]^+$, possibly by reaction with $[D_7]$DMF or $(CD_3)_2$NH/CO, was noted during the approximately 30 minute runs and data was corrected accordingly. At above about 120 °C decomposition was extensive and data became somewhat unreliable. For each cycle in the D_2-array, four dummy pulse-sequences were applied followed by eight acquisition sequences, with a 10 s delay between sequences. The 28 FID in the array were processed and phased in parallel and then peak-heights determined by projection of the array on an arbitrary scale. Values for apparent percentage unmagnetised [*meso*] in the mixture against delay time were extracted using *K* values (determined by van't Hoff analysis), difference in peak height of the [*meso*] isomer from that at $D_2 = 2$ ms) and, if necessary, corrected for the any decomposition occurring during the run-time.

Analysis of kinetics and thermodynamics: Equilibrium values (*K*) between [DL] and [*meso*] were determined by ^{13}C NMR (100 MHz) between +70 and −50 °C allowing reasonable time for establishing complete equilibrium and a van't Hoff relationship, $\ln K_{eq} = 853.3/T - 0.742$ ($r^2 = 0.981$) was determined by linear regression. Kinetics were simulated by using an iterative GEAR procedure, running on MacKinetics.[39] Errors in first-order rate constants (*k*) for rapid temperature drop experiments were estimated by weighted linear regression of plots of ln([DL]eq-[DL]*t*) versus *t* (time [s]). Errors in *k* for the magnetisation transfer simulations were estimated by manually increasing and decreasing the rate (without altering *K* or τ_1) until the fit became visibly unsatisfactory. By using the estimated errors in *k* and in *T*, $\ln(k_{max}/T_{min})$ and $\ln(k_{min}/T_{max})$ were used to calculate errors in data points for the Eyring analyses and then an error-weighted linear regression analysis performed for $\ln(k_{obs}/T) = \ln(h/k_B) - (\Delta H^{\neq}/RT) + \Delta S^{\neq}/R)$ to provide values and confidence limits in the entropic and enthalpic contributions to the overall free energy.

Acknowledgement

G.C.L.-J. thanks Pfizer Ltd and the Zeneca Strategic Research Fund for generous donations and the Nuffield Foundation for a start-up grant (SCI/180/96/142). R.L.W. thanks Pfizer Ltd for a vacation bursary and for continued support in the form of a CASE award. Professor Gary R. Weisman (University of New Hampshire, USA) and Professor Roger W. Alder (Bristol) were most encouraging and informative in discussions regarding structures and stereodynamics.

[1] Bond energies at the higher end of this scale occur almost exclusively in the gas phase, for example, for $[F\text{-}H\text{-}F]^-$ the bond energy is in the range 36–60 kcal mol^{-1}.

[2] G. A. Jeffrey, *An Introduction to Hydrogen Bonding*, Oxford University Press, NY & Oxford, **1997**, pp. 11–32.

[3] R. W. Alder, P. S. Bowman, W. R. S. Steele, D. R. Winterman, *J. Chem. Soc. Chem. Commun.* **1968**, 723–724.

[4] Reviews: a) H. A. Staab, T. Saupe, *Angew. Chem.* **1988**, *100*, 895; *Angew. Chem. Int. Ed. Engl.* **1988**, *27*, 865–879; b) A. F. Pozharskii, *Russ. Chem Rev.* **1998**, *67*, 1–24.

[5] C. L. Perrin, J. B. Nielson, *Ann. Rev. Phys. Chem.* **1997**, *48*, 511–544; C. L. Perrin, J. B. Nielson, Y. J. Kim, *Ber. Bunsenges. Phys. Chem.* **1998**, *102*, 403–409.

[6] For leading references see: a) Y. Kim, S. Lim, Y. Kim, *J. Phys. Chem. A* **1999**, *103*, 6632–6637; b) J. Elguero, *J. Phys. Chem. A* **1999**, *103*, 272–279; c) B. Schitt, B. B. Iversen, G. K. H. Madsen, T. C. Bruice, *J. Am. Chem. Soc.* **1998**, *120*, 12117–12124; d) W. W. Cleland, M. M. Kreevoy, *Science* **1994**, *264*, 1887–1890.

[7] a) J. A. Gerlt, M. M. Kreevoy, W. W. Cleland, P. A. Frey, *Chem. Biol.* **1997**, *4*, 259–267; b) J. P. Guthrie, *Chem. Biol.* **1996**, *3*, 163–170.

[8] a) G. H. Barnett, F. Hibbert, *J. Am. Chem. Soc.* **1984**, *106*, 2080–2084 and references therein; b) A. J. Kresge, M. F. Powell, *J. Am. Chem. Soc.* **1981**, *103*, 972–973.

[9] However, Guthrie (see Reference [7b]) has noted that a similiar hydrogen bond should also be present in $[\mathbf{1b}H]^+$ and proposed that the high basicity of **1a** versus **1b** is more likely to be due to relief of the steric strain present in **1a** and not the formation of hydrogen bonds with very different strength. Based on the data presented herein, we draw a similar conclusion.

[10] Some are of the opinion that this 'special' condition results in a stronger hydrogen bond, however, for some systems at least, it has been shown that there is a linear relationship between hydrogen bond strength and ΔpK_a (i.e. the $\Delta pK_a = 0$ condition is not special). For discussion see: K. N. Houk, *J. Org. Chem.* **1998**, *63*, 4611–4619.

[11] a) C. López, P. Lorente, R. M. Claramunt, J. Marín, C. Foces-Foces, A. L. Llamas-Saiz, J. Elguero, H.-H. Limbach, *Ber. Bunsenges. Phys. Chem.* **1998**, *102*, 414–418; b) G. A. Kumar, M. A. McAlister, *J. Org. Chem.* **1998**, *63*, 6968–6972.

[12] F. Hibbert, *J. Chem. Soc. Perkin Trans II* **1974**, 1862–1866

[13] For leading references on the numerous X-ray structures of $[\mathbf{1a}H]^+[X]^-$, see: C. López, P. Lorente, R. M. Claramunt, A. L. Llamas-Saiz, C. Foces-Foces, J. Elguero, I. Sobrados, F. Aguilar-Parrilla, H.-H. Limbach, *New. J. Chem.* **1996**, *20*, 523–536.

[14] However, some asymmetry in the "strong hydrogen bond" is also noted by ^{15}N NMR spectroscopy, see: C. López, P. Lorente, R. M. Claramunt, J. Marín, C. Foces-Foces, A. L. Llamas-Saiz, J. Elguero, H.-H. Limbach, *Ber. Bunsenges. Phys. Chem.* **1998**, *102*, 414–418 and references therein.

[15] A value of 0.9 has been reported by A. J. Kresge et al., see reference [5] in F. Hibbert, H. J. Robbins, *Chem. Commun.* **1980**, 141–142.

[16] J. A. Platts, S. T. Howard, K. Wozniak, *J. Org. Chem.* **1994**, *59*, 4647–4651.

[17] a) J. P. H. Charmant, G. C. Lloyd-Jones, T. M. Peakman, R. L. Woodward, *Tetrahedron Lett.* **1998**, *39*, 4733–4736; b) J. P. H. Charmant, G. C. Lloyd-Jones, T. M. Peakman, R. L. Woodward, *Eur. J. Org. Chem.* **1999**, 2501–2510.

[18] G. Gunnarsson, H. Wennerström, W. Egon, S. Forsén, *Chem. Phys. Lett.* **1976**, *38*, 96–99.

[19] S. Humble, C. J. Hlakides, J. D. Keltner, M. Messina, *Chem. Phys. Lett.* **1998**, *289*, 90–96.

[20] C. L. Perrin, J. B. Nielson, *J. Am. Chem. Soc.* **1997**, *119*, 12734–12741.

[21] K. G. Orrell, V. Sik, D. Stephenson, *Prog. NMR Spectroscopy* **1990**, *22*, 141–208.

[22] $[D_7]$DMF was employed to allow as wide a temperature range as possible with appropriate solubility for $[\mathbf{2H}]^+$ and compatibility with **2**.

[23] For a discussion of systematic errors and inaccuracies in DNMR see, for example: a) H. Günther, in *NMR spectroscopy*, 2nd ed., Wiley, Chichester, **1995**; b) J Sandström, *Dynamic NMR Spectroscopy*, Academic Press, London, **1982**.

[24] Single crystals were powdered in the bottom of the NMR tube with the end of a glass capillary that had been rounded by melting. Care was taken so that grinding in the solid state would not induce thermal equilibration. The NMR tube was then immersed in an octane-dry ice cooling bath, solvent added and the rounded capillary used to agitate the mixture until dissolution was complete.

[25] Reaction of **3** with dry CD_3I generates $[D_3]$-$[\mathbf{2H}]^+I^-$ which is fully equilibrated *as it is generated*. Any water in the reaction system at the start is sequestered by precipitation with the salt and thus in the latter stages of reaction the system is essentially anhydrous.

[26] E. Havinga, *Biochem. Biophys. Acta* **1954**, *13*, 171–174.

[27] a) The difference in pK_a between **2** and **1a** should be small (e.g. no more than 1 or 2 units) see reference [4b]. b) We attempted to estimate the pK_a of **2** by ^{1}H NMR spectroscopy measurement of the equilibrium proton distribution after mixing equimolar quantities of $\mathbf{2}H^+$ and **1**. However, the measurement was complicated by a side reaction that resulted in extensive debenzylation.

[28] Evidently, the diastereoisomers cannot directly interconvert since the hydrogen bond must be broken before or during the process and then reformed. In other words the hydrogen is acting as a lock (albeit inefficient). See also reference [30].

[29] F. Hibbert, *Acc. Chem. Res.* **1984**, *17*, 115 – 120.
[30] M. Saunders, F. Yamada, *J. Am. Chem. Soc.* **1963**, *85*, 1882.
[31] We are still trying to prepare **6**. However, thus far eight different synthetic routes have been devised and tested. All have proved unsuccessful and this attests to the steric congestion of such a system.
[32] Entropy of mixing of enantiomers and entropy of symmetry should cancel, see: E. L. Eliel, S. H. Wilen, L. N. Mander, *The Stereochemistry of Organic Compounds*, Wiley, Chichester, **1994**. The exchange rates were found to be constant over a two-fold concentration range of [**2**H]$^+$ and the process is thus unimolecular or pseudounimolecular.
[33] F. Hibbert, K. P. P. Hunte, *J. Chem. Soc. Perkin Trans II* **1983**, 1895 – 1899.
[34] R. W. Alder, *Chem. Rev.* **1989**, *89*, 1215 – 1223.
[35] If a two stage mechanism (Schemes 2 and 3) is in operation, $k_{obs} = k_2K_1$. Thus, if $k_2 = k_2'$, since $k = (\kappa k_B T/h)[\exp(-(\Delta G/RT)]$ and assuming the transmission coefficients are close to unity then $K_1 = \exp[-(\Delta G_{obs} - \Delta G_2)/RT]$. Thus, in DMF at 298 K, $K_1^{[DL]} =$ ca. 1.4×10^{-5} and $K_1^{[meso]} =$ ca. 4.7×10^{-5}. These results are reasonably close to the value of 6×10^{-6} found by Hibbert for [**1a**H]$^+$.[12].
[36] An estimate of the hydrogen bond energy ($\Delta G^{\ddagger}_{298}$) of 6.5 kcal mol^{-1} was made.[8]
[37] a) M. L. Kaplan, F. A. Bovey, H. N. Cheng, *Anal. Chem.* **1975**, *47*, 1703 – 1705; b) A. L. Van Geet, *Anal. Chem.* **1970**, *42*, 679 – 680.
[38] T. D. W. Claridge, *High-Resolution NMR Techniques in Organic Chemistry*, Pergamon, Elsevier Science, Oxford, **1999**.
[39] Commercial software (Leipold Associates, USA).

Received: May 8, 2000 [F2472]

 © WILEY-VCH Verlag GmbH, D-69451 Weinheim, 2000 0947-6539/00/0624-4460 $ 17.50+.50/0